Progress in Additive Manufacturing (2026) 11:1689–1703
https://doi.org/10.1007/s40964-025-01435-4

RESEARCH

Additive remanufacturing (AReM): integrated product-process design for functional upgrades of existing components by directed energy deposition

Enrico Dalpadulo[1] · Fabio Pini[1] · Francesco Leali[1]

Received: 28 August 2025 / Accepted: 20 November 2025 / Published online: 8 January 2026

Abstract

Directed Energy Deposition (DED) is increasingly utilized for the construction of large components, repair of worn and damaged parts, and integration into Hybrid Manufacturing systems to leverage diverse technological features. A burgeoning application of DED is in Additive Remanufacturing (ARem), by which existing components can be enhanced with additional features and materials to improve functionalities. This paper presents a systematic and integrated approach for Design for Additive Remanufacturing (DARem), focusing on the optimization of product structural requirements to enhance performance and the process design to minimize flaws while ensuring material integrity and expected tolerances.

The suggested approach involves product and process design phases within a computer aided design platform. Identification of critical issues in the original product design is the fundamental phase that drives the selection of the appropriate materials and quantities for deposition. Next, topological optimization is employed to shape and position additional volumes, generating enhanced design variants. A simulation phase ends the product design steps, assessing the actual improvement of the component over its original design.

Subsequent phases are related to process design assessment. Selection of process parameters and build strategies, and next, the behavioral simulation of deposition are fundamental to verify feasibility and generate paths instructions. Finally, thermomechanical simulation is conducted to estimate the final component state accurately, ensuring it meets functional requirements before proceeding to actual manufacturing pre-processing, material deposition, and post-processing phases.

A case study involving an automotive suspension component is used to demonstrate the feasibility of the proposed integrated approach. Experimental phases are performed to define DED material properties for the redesign and investigate the reliable simulation of process-induced distortions. By reducing stress in critical areas through localized deposition of 316L stainless steel alloy using laser powder DED, the study explores the impact of toolpath strategies on process-induced distortions through a Design of Experiments (DoE) approach. The results confirm the feasibility of the deposition process in meeting functional requirements, particularly geometrical tolerances, highlighting the potential of DARem for the redesign and enhancement of existing components. This integrated approach not only consolidates remanufacturing procedures but also promotes the use of simulation tools to preemptively address potential issues, ensuring efficient, one-shot component creation.

Keywords Directed Energy Deposition · 316L, Remanufacturing · Product-Process design · Finite Element Method

✉ Enrico Dalpadulo
enrico.dalpadulo@unimore.it

Fabio Pini
fabio.pini@unimore.it

Francesco Leali
francesco.leali@unimore.it

[1] Enzo Ferrari Department of Engineering, University of Modena and Reggio Emilia, Modena, Italy

1 Introduction

Metal Additive Manufacturing (MAM) is increasingly adopted in high-end industries within the Industry 4.0 framework. Among the various MAM technologies, Powder Bed Fusion (PBF) [1][ISO/ASTM52900:2021] is prominent, enabling the creation of geometries characterized by high geometrical complexity and offering significant

design flexibility. This capability supports the development of innovative functional products through Design for Additive Manufacturing (DfAM) strategies [2]V[Ngo 2018]. Directed Energy Deposition (DED) [ISO/ASTM 52900:2021] systems (Fig. 1) offer a compelling alternative in MAM, characterized by high deposition rates, large build volumes, high manufacturing flexibility, and the capability to process multi-materials and graded materials [3]. Firstly, DED is therefore particularly suitable for large-scale applications in sectors like aerospace and construction, where it is commonly used to manufacture extensive metal structures [4]. Integration with robotic systems further enhances its potential for creating some of the largest additively manufactured components [5][OpenElectronics]. Moreover, its cost and lead-time efficiency contribute to sustainable product development, as evidenced in automotive applications like the Red Bull Racing car drivetrain and suspension system [6]. Despite such benefits, DED has limitations in resolution and design flexibility, restricting its application to simpler geometries. Nevertheless, DED has the ability to engineer Functionally Graded Materials (FGMs), enabling the development of components with enhanced properties, such as improved wear resistance, hardness, corrosion resistance, and thermal performance [7]. Moreover, DED is also valuable for repairing damaged parts, remanufacturing existing components, and even producing functional design variants [8]. Finally, DED process is increasingly utilized in hybrid manufacturing systems, combining the strengths of multiple technologies. Hybrid Additive Manufacturing (HAM) integrates construction and finishing phases within numerical control or robotic systems, offering benefits such as improved mechanical and surface properties, as well as significant time and cost savings [9].

1.1 Repair, reconditioning, and remanufacturing

The literature review by Piscopo et al. highlighted repair and maintenance as the primary applications of DED technology, particularly in the aerospace sector [7]. It is also extensively utilized for repairing tools and molds, as well as in the automotive, marine, and railway industries [7].

In fact, Repair, Reconditioning, and Remanufacturing contribute significantly to greater sustainability by extending the lifecycle of components while minimizing resource consumption. Each approach achieves this in distinct ways:

- Repair focuses on restoring a damaged component to functionality, though the repaired part rarely matches the original in performance. Typically, only the repaired area is guaranteed to meet specific standards. Examples of successful repairs include turbine blades [10] [Gesser, 2010]; [11] and engine components like cylinder heads [12] or crankshafts [13].
- Reconditioning involves processing a component to restore its performance to that of a new or nearly new product. Unlike repair, reconditioning ensures the functionality of the entire component, albeit with performance that might occasionally be slightly below original standards. This method is particularly effective for molds [14] and dies] [15] [Bennett, 2019], where processes have been specifically developed to restore these tools.
- Remanufacturing goes beyond repair and reconditioning by creating a product that is "as good as new" or even "better than new" when upgrades are introduced during the process. It is an effective strategy to counteract obsolescence or address unforeseen design issues [16].

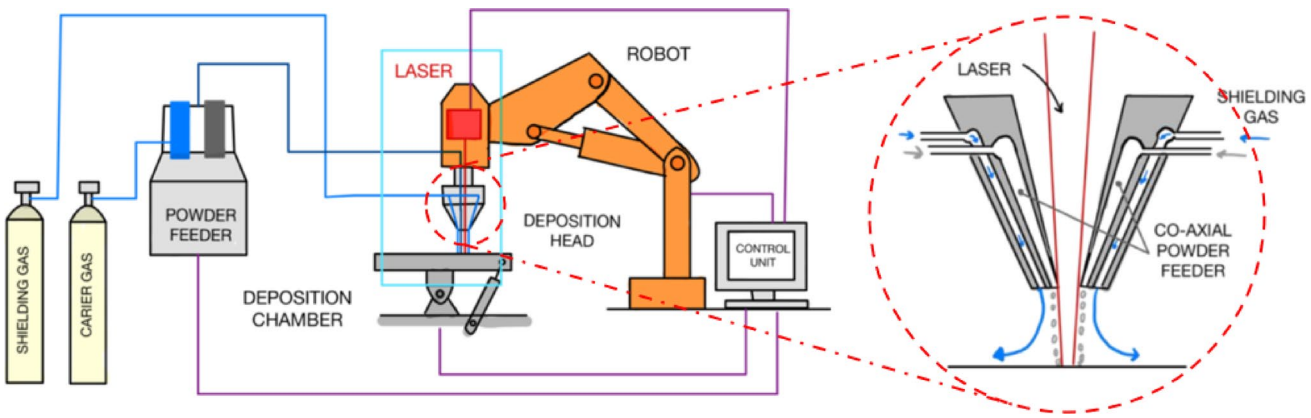

Fig. 1 A Laser based DED (DED-LB) system, where a laser acts as energy source, the material feed is provided by gas-assisted powder, and the deposition is performed by a robotic arm, which can be integrated with a workpiece table into a workcell

1.2 Additive remanufacturing

Furthermore, a related emerging application is Additive Remanufacturing (AReM), which focuses on enhancing existing components by incorporating new features and materials to improve functionality. For example, mechanical resistance, stiffness, or fatigue life of a part can be improved. Also, new features can be added to create design variants, implement quick design changes, or to enhance further characteristics, such as heat dissipation or corrosion resistance, even exploiting multi-materials. This approach aims to retain original production materials and equipment while adding value through customization. The potential of AReM has been demonstrated in limited cases, including the construction and reinforcement of customized parts as reported by Hedges et al., Polenz et al., and Josten et al. [Hedges 2006, [17, 18].

AReM adoption in industrial environments faces challenges due to the complexity of design strategies, geometric constraints, and process parameters selection and thermal management.

DfAM research needs for specific approaches to overcome such issues and enhance actual AM capabilities [19–22]. This research addresses the absence of a comprehensive, reproducible framework for the ARem implementation via DED. By proposing a structured Design for Additive Remanufacturing (DARem) systematic approach, this work facilitates simulation-driven product/process design integration, promoting reliable and effective remanufacturing solutions. The next section describes the approach and the tools suggested for the implementation. The use case selected to demonstrate the feasibility of the approach is presented in Sect. 3. Section 4 provides the results achieved, and Sect. 5 ends the paper with the conclusions and an overview of potential further improvement directions.

2 Method and tools

The DARem methodology is based on the deposition of multiple optimized geometries (hereafter Depositions) to achieve component performance enhancement. The approach is articulated across the two major computer-based phases Product Study and Process Study each further subdivided into specific tasks with distinct objectives (Fig. 2). These core phases are included in a wider framework, preceded by a product planning phase and followed by the component manufacturing phase. Redesign loops may be required either for the Product study or the Process study if the project's requirements are not fulfilled. The approach is designed to anticipate functional and process-based issues prior to physical manufacturing, reducing trial-and-error iterations. More details on the phases are provided in the following.

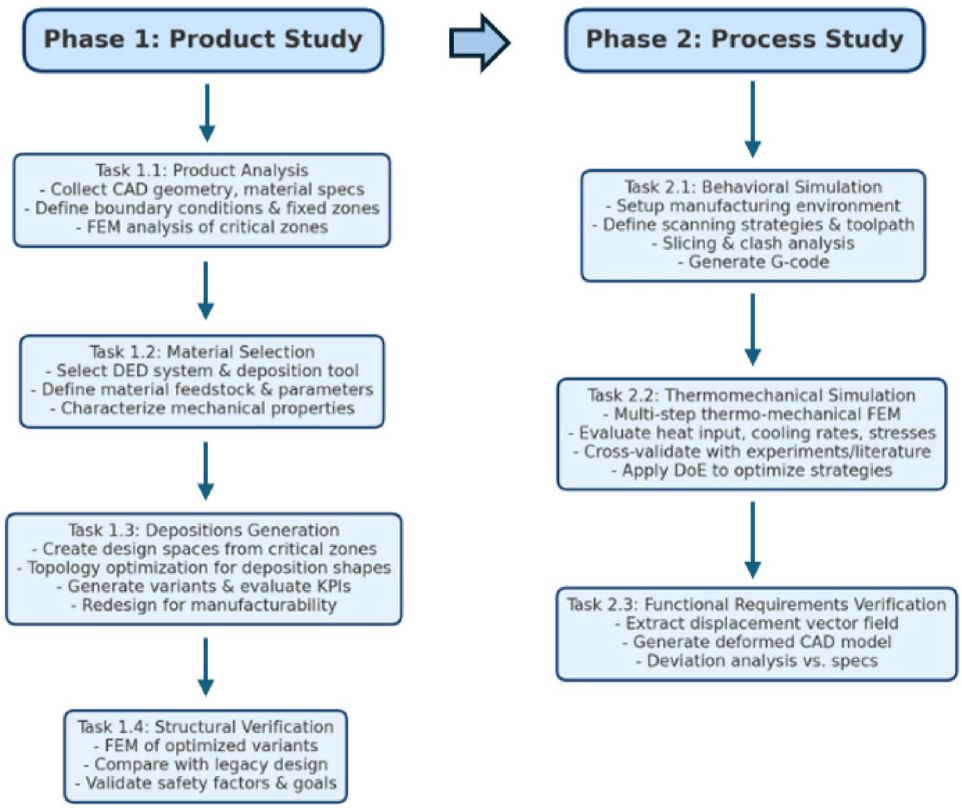

Fig. 2 The DARem methodology and the two core phases Product Study and Process Study

Phase 1: Product study—this is the first design core phase. It is related to product analysis and functional optimization to meet the remanufacturing performance requirements. A total of 4 main sub activities is involved within this phase, that are the 4 design remanufacturing tasks described in the following.

Task 1.1: Product analysis—The initial task focuses on understanding the baseline component. This includes:

- Collection of geometric and material specifications from the 3d product model and technical documentation.
- Definition of boundary conditions (fixtures, load cases, contact interfaces), identification of fixed zones (i.e., where material deposition is not allowed), and depositions target mass.
- Structural FEM analysis to evaluate the mechanical behavior and potential failure points (i.e., critical zones) under operating conditions.

Task 1.2: Material selection—This task involves the selection of the DED system, the related deposition tool, and the characterization of deposition material. This includes:

- Selection of material type, feedstock, characteristics
- Selection of build parameters (power, speed, bead overlaps, etc.)
- Definition of mechanical properties, or experimental characterization

Task 1.3: Depositions generation—The goal of this task is to identify the optimal locations and shapes of the depositions. This includes:

- The creation of Design Spaces, compatible with part assembly constraints. The regions are created on the critical zones highlighted by preliminary structural analysis, returned by task 1.1. The fixed zones or areas that are unreachable by the deposition tool are excluded.
- Topology optimization based on the structural analysis setup, to identify optimal shapes of the depositions given the target mass.
- Generation of several variants and evaluations based on Key Performance Indicators (KPIs) such as mass, stress, and displacement.
- Preliminary re-design of the depositions considering manufacturability aspects (e.g., voids, overhangs, dimensions)

Task 1.4: Structural verification—The aim of this task is the validation of the Product Study in case of compliance with safety factors and the project's goals. This includes:

- Structural FEM analysis of the optimized design variant
- Comparison between the legacy component and the optimized design variants

Phase 2: Process study—This is the second design core phase. It focuses on assessing the manufacturing process in terms of final distortions due to the high thermal fields that are characteristic of DED technologies. 3 sub activities are involved within this phase, listed in the following.

Task 2.1: Behavioral simulation—This task includes the setup of the deposition strategies and the feasibility study preventing potential interferences. This involves:

- Creation of the manufacturing environment, including the virtual machine and the deposition tool, and the positioning of the component on the workpiece table
- Definition of the scanning strategies and creation of the toolpath
- Slicing and clash analyses to validate the toolpath
- Creation of the G-code for additive manufacturing

Task 2.2: Thermomechanical simulation—The goal of this task is to evaluate the deposition process and predict possible manufacturing flaws. This includes:

- Multi-step thermo-mechanical FEM analysis of the deposition, to evaluate the impact of heat input, cooling rates, and material phase transitions, where stress and distortion fields are modeled with boundary conditions reflecting the actual build setup.
- Nonmandatory results cross-validation against experiments or literature
- Possible Design of Experiment (DOE) approach to optimize the deposition strategies

Task 2.3: Functional requirements verification—The aim of this task is the validation of the Process Study by assessing the fulfilment of the functional requirements. This includes:

- Extraction of the nodal displacement vector field from the thermomechanical simulation
- Creation of the deformed CAD model due to the deposition process
- Comparison of the CAD models via deviation analysis to evaluate conformity with respect to geometrical specification

The novelty of DARem methodology is also related to the adoption of a PLM platform environment to support the tasks of the two aforementioned design phases. The purpose is to assume a reference architecture where to exploit the integration between CAD, CAE, and CAM tasks to

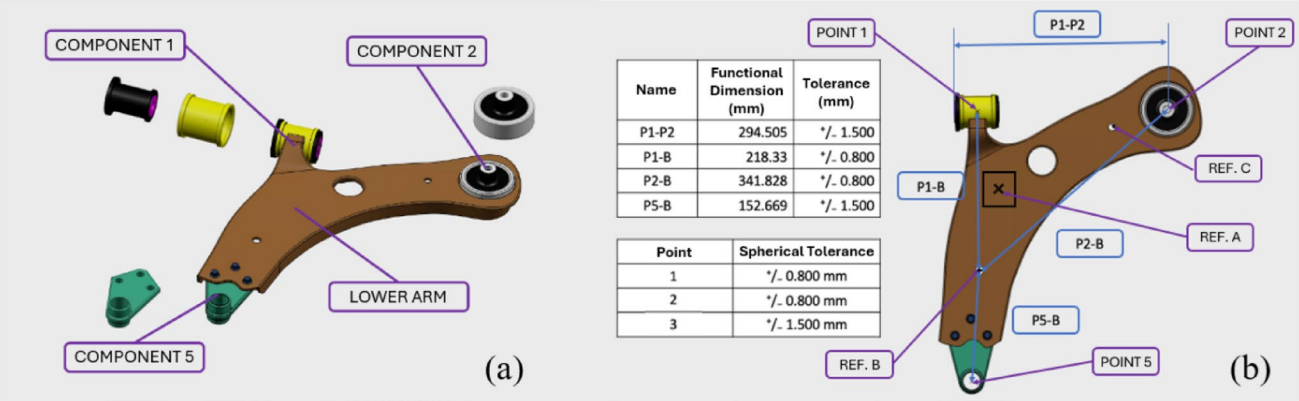

Name	Functional Dimension (mm)	Tolerance (mm)
P1-P2	294.505	*/- 1.500
P1-B	218.33	*/- 0.800
P2-B	341.828	*/- 0.800
P5-B	152.669	*/- 1.500

Point	Spherical Tolerance
1	*/- 0.800 mm
2	*/- 0.800 mm
3	*/- 1.500 mm

Fig. 3 **a** The sub-assembly composed of the arm, 1, 2, and 5, and **b** the functional requirements for Point 1, Point 2, and Point 5.

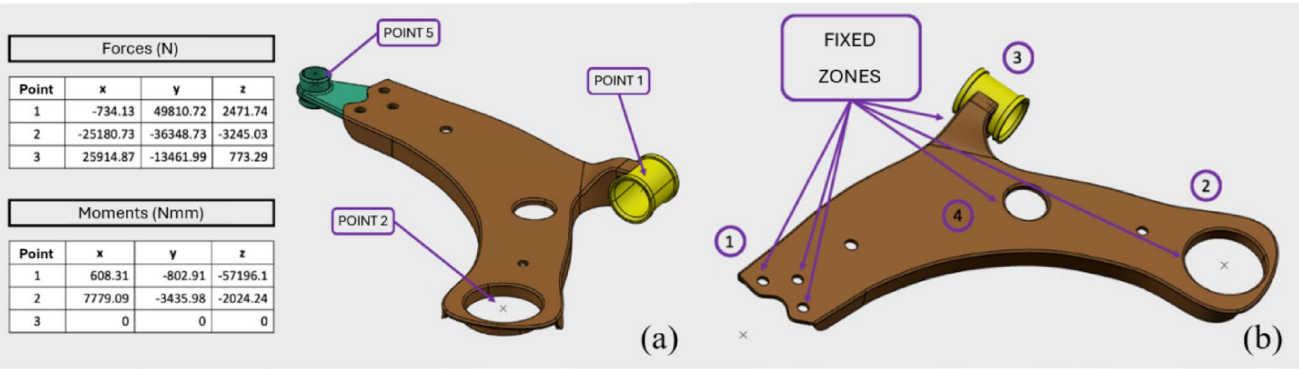

Forces (N)

Point	x	y	z
1	-734.13	49810.72	2471.74
2	-25180.73	-36348.73	-3245.03
3	25914.87	-13461.99	773.29

Moments (Nmm)

Point	x	y	z
1	608.31	-802.91	-57196.1
2	7779.09	-3435.98	-2024.24
3	0	0	0

Fig. 4 The reference load case expressed in vehicle's reference system (**a**), and the fixed zones, where material addition is not allowed (**b**)

seamlessly achieve concurrent product and process design optimization. The selected platform is Dassault Systèmes's 3DExperience, whose modelling tools are Catia, simulation tools are Simulia (using the FEM Abaqus solver), ad manufacturing programming tools are Delmia. The tasks of the methodology have been outlined through synergic design, simulation, and DED-LB experimental studies (e.g., process testing, material characterization, residual distortion assessment), to define a robust and reliable framework which aims to be suitable for industrial implementation. An overall case study, which requires both structural and functional requirements has been selected to illustrate and validate the proposed approach.

3 Case study and methodology implementation

The aim of the case study is to detail and demonstrate the application of the DARem methodology on a lower control arm of a MacPherson suspension system of a B-segment SUV, which is a structural component subjected to high dynamic loads. The goal is not merely to repair the component selected, but mainly to enhance mechanical performance through localized material addition using DED-LB, avoiding complete redesign of the product and replacement of the related manufacturing processes.

Product study: product analysis—Following the stages by the suggested approach, through the first product design task, functional requirements and structural requirements need to be identified. To extract functional requirements, the 3D CAD models and the 2D engineering drawings are analyzed. Moreover, information about the bill of material (BOM), the material, the manufacturing process, and the weight is collected. Specifically to the use case selected, the material is stainless steel, the primary process is cold stamping, and the part weighs 1825 kg. Functional dimensions and related dimensional and geometrical tolerances represent fundamental constraints to fulfill functional assembly requirements. Figure 3a depicts the parts included in the sub-assembly and Fig. 3b highlights the functional dimensions (i.e., P1-P2, P1-B, P2-B, P5-B) and the related tolerances.

Concerning the structural requirements, it is necessary to evaluate the physical behavior of the legacy component and highlight the critical aspects to be improved by DARem to derive the reference information. A structural FEM analysis is set up, with the most critical load case reported in Fig. 4a, that is extracted by a multibody overall simulation of the

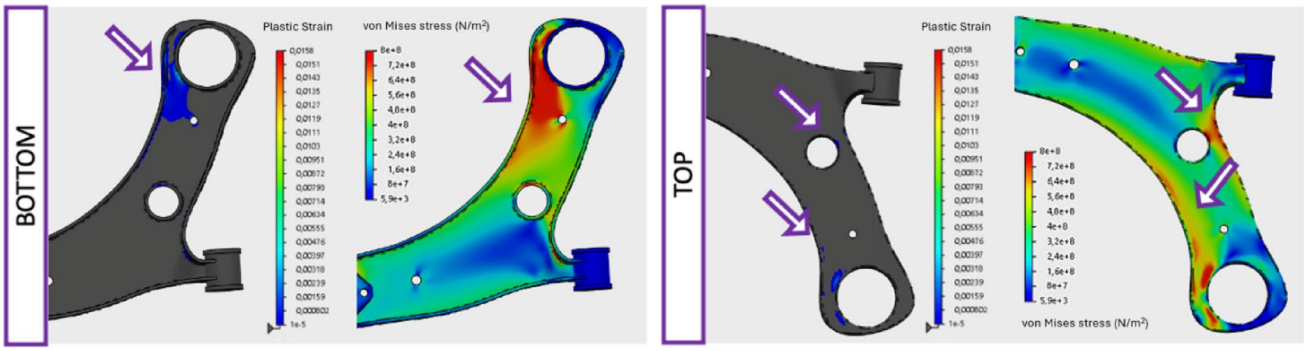

Fig. 5 The structural FEM analysis of the legacy part highlighting which are the critical zones—identified by the arrows

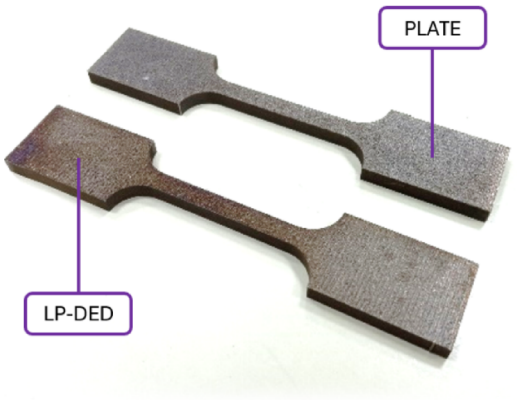

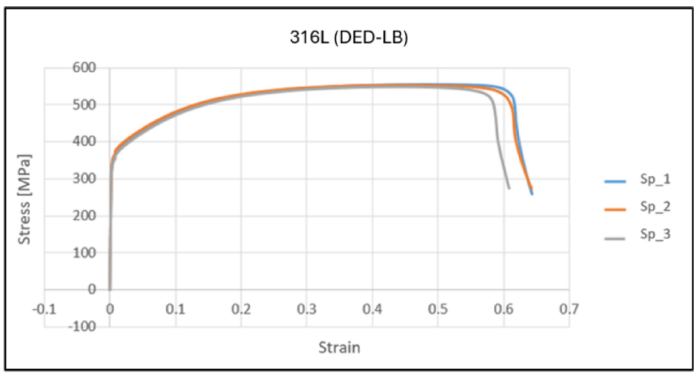

Mechanical properties of 316L (DED-LB)			
E (Gpa)	Y (Mpa)	UTS (Mpa)	e (%)
156.8	343.6	552.6	58.9

Fig. 6 The tensile specimens (left) and the mechanical properties of 316L steel by DED-LB. **b** The bi-material specimens and the related tensile test data (left), and the fracture surface at 80x. Ductile failure characteristics (e.g., transgranular ductile fracture, with dimples and microcavities) could suggest adequate bonding between layers and moderate anisotropy.

suspension mechanism. Afterwards, the aims of this task are to define the zones where material addition is allowed or not, and what the target mass is for the depositions. Figure 4b shows the zones of the components that must be kept unaltered to ensure component fitting, here named as fixed zones and listed as follow: 1. the three holes for fixing component 5; 2. the housing for the interference-fit component 2; 3. the area near the bushing that is secured to the arm by welding; 4. the central hole in the arm.

The definition of the target mass is tied to the critical behavior reported by the FEM analysis. Areas with equivalent von Mises stress close to the ultimate tensile stress (UTS) are found, and two critical zones are recognized (Fig. 5), which are the areas of the model in which plastic strain occurs. In Fig. 5, they are highlighted by setting the von Mises stress threshold to 800 MPa (UTS). A high-performance design variant is created by parametrically increasing the thickness of the plate from 3.5 to 3.7 mm. This allows for the containment of plastic strain within the acceptable range. Since the difference between the legacy design and the high-performance design is 0,096 kg, the target mass available for the material addition is calculated as 0, 1 kg.

Product study: material selection—For remanufacturing purposes, the selected material is the 316L stainless steel, available in powder suitable for DED-LB. The machine selected to perform the process is the LASERDYNE 811 from Prima additive [PrimaAdditive]. Main process parameters were selected based on previous studies with the experimental setup. In fact, they directly affect the quality of the bead, its adhesion and growth with respect to the substrate, its density and potential porosity, microstructural characteristics such as dimension of the grains [23–25]. Hereafter are reported the main process parameters for a laser beam with a focus diameter of 2 mm: Laser Power = 800 W; Scan speed = 800 mm/min; Layer height = 0.5 mm; Hatching distance = 1.2 mm. Once the parameters allowed to obtain beads and depositions with the expected quality have been identified, tensile test specimens were fabricated following the ISO 6892–1 standard (Fig. 6, left) to obtain the corresponding mechanical properties. The additive specimens were built along the Z direction to obtain characteristics in favor of safety. To extract accurate results for FEM material

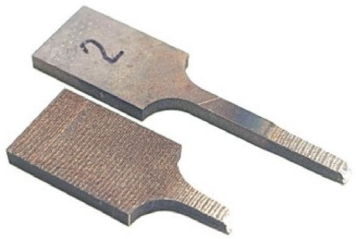

Mechanical properties of the bi-material specimens				
	E (Gpa)	Y (Mpa)	UTS (Mpa)	e (%)
1	183	356	553	11.6
2	185	368	564	22.2
3	171	361	565	24.3
4	183	370	563	18.3
5	184	363	562	30.1
AVG	181.2	363.6	561.4	21.3

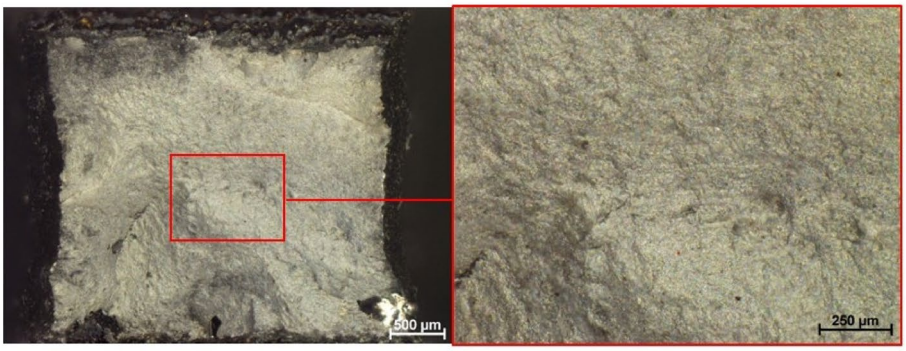

Fig. 7 The bi-material specimens and the related tensile test data (left), and the fracture surface at 80x. Ductile failure characteristics (e.g., transgranular ductile fracture, with dimples and microcavities) could suggest adequate bonding between layers and moderate anisotropy.

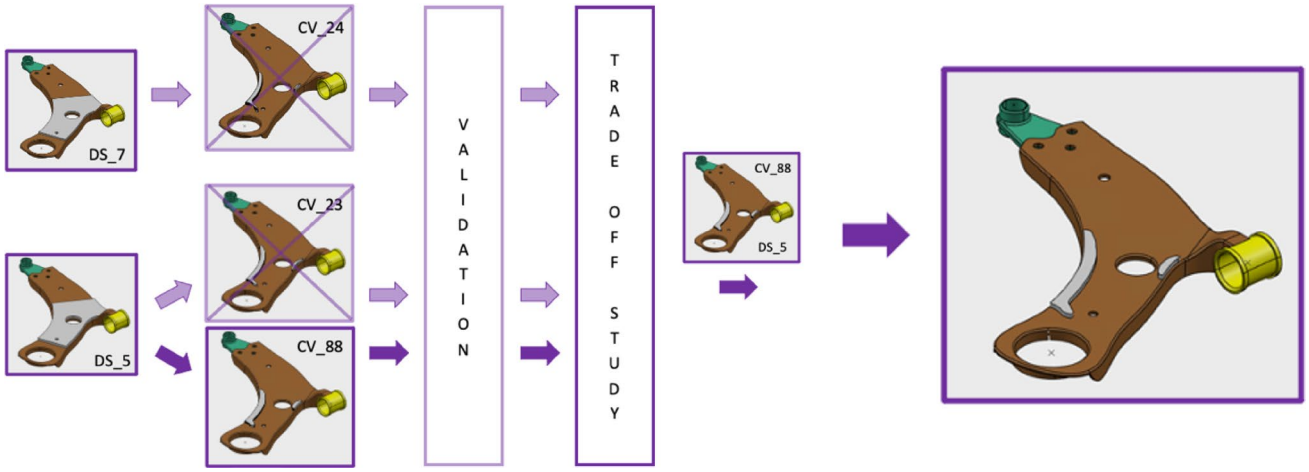

Fig. 8 The stages of the depositions generation (left to right): creation of the design spaces on the critical areas; creation of design variants through topology optimization; trade-off and selection of the best result; redesign of the result to obtain depositions with manufacturable shapes

cards, specimens for both the additive material and the plate material of the lower arm (which data is reserved) were created, keeping the same nominal thickness. Tensile tests were performed using an Instron 6658 system equipped with a 30 kN load cell. Figure 6 (right) reports the stress–strain curve and the mechanical properties of 316L, whereas those of the plate are reserved. A remark is that the correct bonding between the deposition and the substrate is crucial. Figure 7 (left) shows additional bi-material specimens, from which excellent bonding can be observed. In fact, the fracture (Fig. 7, right) occurs always in the DED-LB material, as well as for every specimen Y and UTS are greater compared to 316L.

Product study: depositions generation—The aim of this task is to understand the location and the shape of the depositions. This design strategy was retrieved by the approach developed in [26] [Reference A]. The approach is based on a tailored use of topology optimization techniques. The result of the FEM analysis performed in the initial task drives the positioning of Design Spaces, which are located on the critical zones. Subsequently, Design Spaces must be created according to the physical constraints of the assembly in static and kinematic conditions. Two Design Spaces were created, selecting respectively a 5 mm (DS_5) and a 7 mm (DS_7) height, as visible in Fig. 8 (left). Afterwards, a topology optimization case is set up. Particularly, it is created within a multi-body environment, where the part and the Design Space are linked by tie connections. The parts are discretized by tetrahedron meshes, quadratic for the arm (TET-10) and linear for the Design Space (TET-4), and the corresponding materials are assigned. A SIMP method is set for topology optimization, with a target mass of 0.1 kg and a constraint of 5° overhang angle. Some design variants are created and compared using structural KPIs and the result providing the highest score is preliminary redesigned considering manufacturability by DED (Fig. 8, right).

Product study: structural verification—A structural FEM analysis case is created for the optimized part, retrieving the

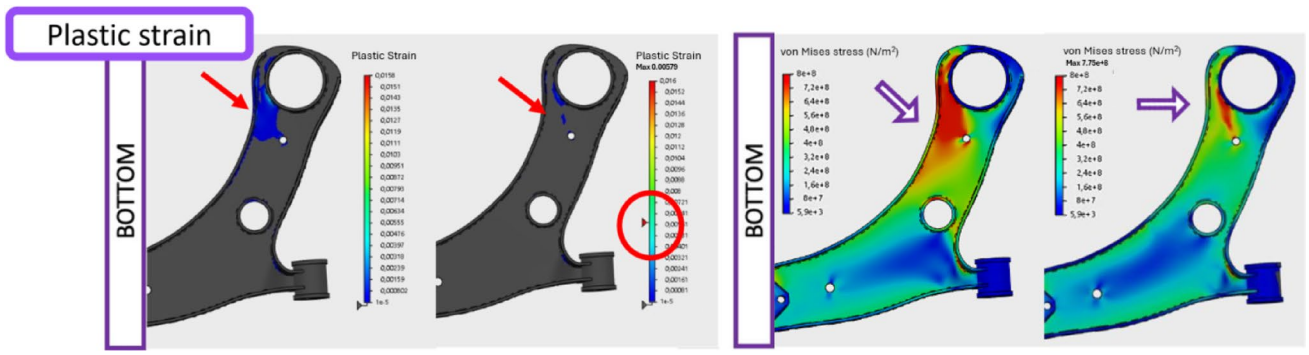

Fig. 9 The reduction of plastic strain at the bottom of the arm (left), and the stress state improvement (right)

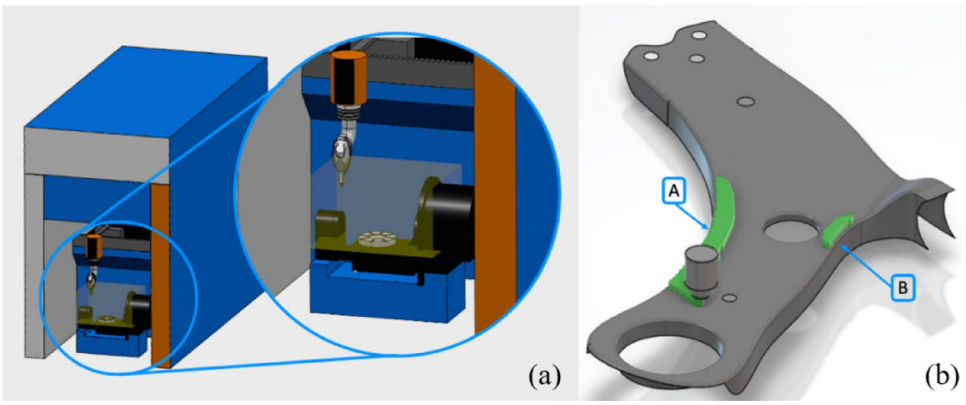

Fig. 10 The digital twin of the LASERDYNE 811 by Prima Additive (**a**) and the schematics of depositions A and B for which the tool path must be generated (**b**)

setup of the load case used for the simulation of the legacy part. The plastic strain is the parameter selected to compare the two design variants and evaluate the enhancement of the component. As reported in Fig. 9 the analyses can be compared. Therefore, (i) the maximum plastic strain is reduced by one order of magnitude, the extension of the areas with plastic strain is highly reduced, and (ii) the equivalent von Mises stress is also lower than UTS in the previously identified critical zones. In particular, Fig. 9 (right) highlights the reduction of plastic strain at the bottom of the arm, which was reported as the most critical issue.

Process study: behavioral Simulation—To start the process study phase, the manufacturing virtual environment is created, including a virtual replica of the machine, the deposition tool, and the associated build parameters. Figure 10a shows the digital machining environment of the Laserdyne 811, which is not just a 3D kinematic model, but allows for programming and virtual testing. The deposition tool is set to reflect actual parameters and measurements: Tool power = 800 W; Deposition speed = 800 mm/min; Bead width = 2.4 mm; Bead height = 0.5 mm. The component is positioned in the machine, and the tool path generation is performed for the two depositions, namely A and B (Fig. 10b). About the build strategies, they have been identified by means of a DOE, which is reported in next section. The build program can be created, and the process can therefore be simulated and validated if clashes and/or singularities do not occur.

Product study: Thermomechanical simulation—The thermo-mechanical FEM analysis is a key step in the approach to prevent process-related issues, in particular process-induced distortions that can compromise product functional requirements [27] [Liang 2018]. The analysis setup tailored for DAReM by DED-LB was preliminary developed in [28]. To enable fast computation with actual parts, the arm is modeled with quadrilateral shell mesh. A required calibration is performed with respect to experimental data, obtained with a laser scanner Konica Minolta Range 7 characterized by a certified VDI/VDE 2634 accuracy of ± 40 µm. Figure 11 (left) reports the comparison between experiments and simulation, where the deformation of the substrate (represented by the actual component) is measured. A total of five (n = 5) replicate 40 × 40 × 5 mm 316L depositions on 100 × 100 × 4 mm steel substrates were produced. The acquired point clouds were aligned constraining the clamping region of the specimen, maximum out-of-plane displacement were found as mean = 0.603 mm and σ = 0.007 mm. The calibrated shell-based FEM model reproduced the same deformation trend, yielding predicted displacements with a mean absolute deviation of 0.020 mm (≈3%), which falls within the scanner's measurement uncertainty. The multi-step analysis replicates three phases: Deposition;

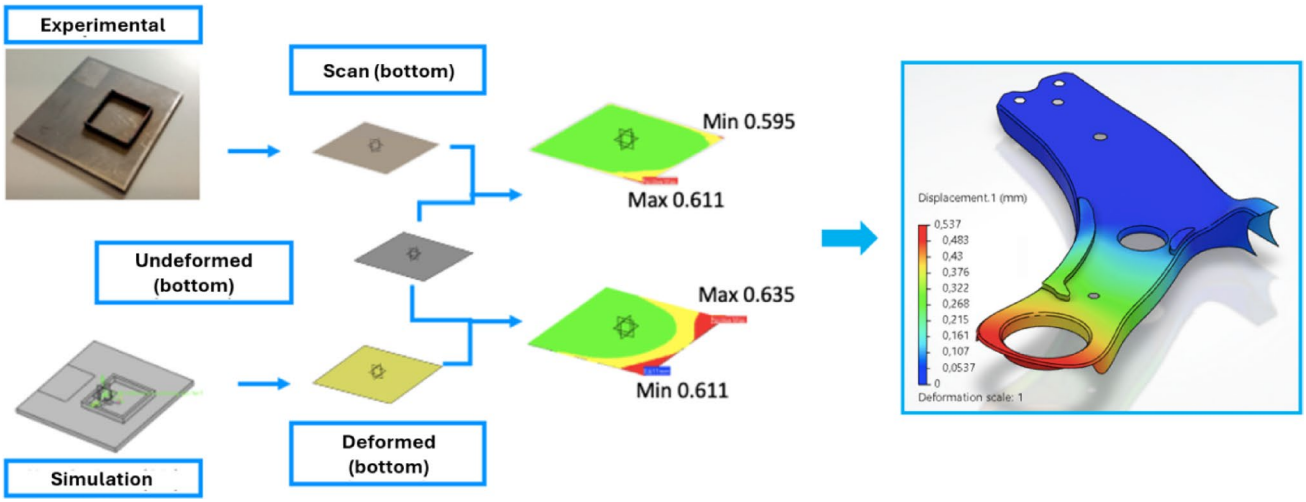

Fig. 11 On the left, the calibration procedure and the deviation analyses performed to compare results from experimental and simulated data with the nominal (undeformed) geometry. On the right, the result of the mechanical step after unclamping for a given build strategy

Table 1 The main parameters of the thermo-mechanical FEM analysis

FEA	Settings
Plate mesh	4 mm 2D quad
Depositions mesh	(0.8 × 0.8 × 0.5—Z) mm 3D hexa
Deposition timestep	Duration: Build strategy; Increments: 1 s
Deposition boundary conditions	Initial T = 300 K; Convection coefficient = 18 W/kg·m^2; Radiation emissivity = 0.25
Energy source	Uniform, 2 mm
Cooling timestep	Duration: 1200 s; Increments: (20–60) s
Unclamping timestep	Duration: 30 s; Increments: 10 s
Virtual bolt	Ref. B nodes translations

Cooling; Unclamping. For the Deposition step, data for the concurrent heat source movement and mesh activation are automatically retrieved by the program generated in the previous task, allowing for seamless tool path generation and simulation. A virtual bolt to replicate the fixture system is activated for the Deposition and Cooling steps, and removed for the Unclamping. Regarding the depositions' mesh, a sensitivity analysis allowed to discretize each bead cross section, whose width and height are approximately 2.4 and 0.5 mm, with three elements of (0.8 × 0.8 × 0.5) mm. Table 1 reports main simulation parameters, whereas materials' thermo-mechanical properties can be found in Appendix A.

Design of experiment—The selection of the build strategies is supported by a DOE approach fully described in [29]. In fact, scientific literature provides many studies regarding DED process parameters optimization, and a few about deposition strategies on simple geometries [30–33]. Nevertheless, it lacks approaches dealing with complex or multiple geometries, and their interaction with the substrate, which is represented by the actual component. The effects of discrete factors such as deposition strategy, orientation, direction, and sequence, and their interactions, were investigated through DOE [34]. For each run, the model maximum displacement calculated by the thermo-mechanical FEM analysis was the primary response, and the build time obtained by the behavioral simulation was the secondary one. Therefore, for multiple depositions characterized by aspect-ratios ≠ 1, the study revealed the optimal build strategy as reported in Fig. 12. The DOE approach is synthesized in Appendix

- Scanning sequence: B-A (in sequence, the largest deposition last)
- Scanning pattern: Line patterns
- Scanning pattern direction: Bidirectional (forth and back)
- Scanning pattern orientation: 90° (parallel to the shortest dimension)

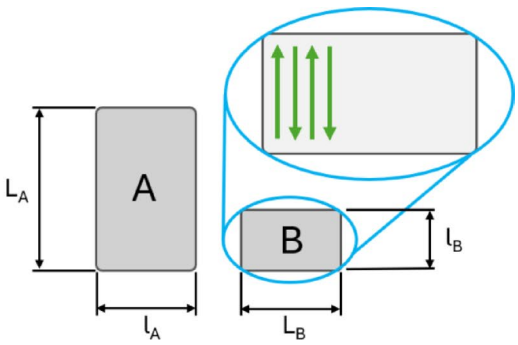

Fig. 12 The optimized factor combination and the related schematic

B. Interestingly, not only the direction of the scanning pattern but also the scanning sequence are highly influential, therefore long deposition tracks should be avoided as well as simultaneous (in-parallel) build of the depositions [34].

Product study: Functional requirements verification—The nominal geometry and the model with the process-induced distortions must be compared in their functional dimensions and tolerances. The nodal displacement vector field (Fig. 13a) is extracted from the thermo-mechanical FEM analysis, and it is applied to the 3D model to obtain the deformed geometry. To perform the measurements, it is essential to align the objects by using the datum system of the part, where plane A orients, axis B locates, and point C locks. Figure 13b shows the overlapping models after the alignment procedure with the datums. Figure 13c shows the verification procedure for the position of point 1, point 2, and point 5, considering the spherical tolerance zones. The part to be produced with the optimized process provides the following dimensions: P1-P2 = 294.388 mm; P1-B = 218.39 mm; P2-B = 341.981 mm; P5-B = 152.672 mm.

4 Discussion

A holistic methodology for DARem was proposed, with the aims to design effective functional upgrades of existing components exploiting material addition, but also to provide the associated process via DED preventing possible flaws. The approach exploits proper numerical simulations to drive both the tasks for product optimization and process optimization, thus meeting the functional requirements.

As a case study, an automotive suspension arm was designed for DARem, to obtain structural reinforcement of a legacy part without replacing materials, manufacturing processes and related hard tooling. The product analysis yielded two objectives, which are (i) structural requirements and (ii) functional requirements. Structural requirements are expressed with the stress state of the part and are evaluated by the reduction of the plastic strain; whereas functional requirements deal with the correct assembly and performance of the suspension system and are evaluated by the compliance with tolerances. A structural FEM analysis is used to highlight the critical zones and determine the location of the depositions. A topology optimization is performed within design spaces positioned on the critical zones, to define the shape of the depositions. After a preliminary redesign to ensure manufacturability via DED, the legacy part and the optimized design are compared. In the arm, the stress areas are reduced, and the maximum equivalent von Mises stress is brought below the material yield stress. The extension of the area where the plastic strain is greater than $1e^{-5}$ is reduced by almost 90%. Also, the maximum value of plastic strain is reduced by over 50%. Regarding the deposition process, the thermo-mechanical FEM analysis allows to assess the residual stress and deformation, which can compromise functionality. The study performed with the DOE approach, assessing main build parameters, provide deformations ranging within one order of magnitude, from 0.3 to over 3 mm. This confirms the fact that the heating and cooling thermal history is influential when high thermal gradients are involved. In fact, with material addition, vertical periodicity is relevant and simultaneous build of multiple depositions should be avoided. The optimal combination of build parameters is the input for the process study, where the tool path is generated and the process is simulated. The deformed geometry is created and finally assessed within the verification task, where three functional points were measured. Respectively, P1 shifts by 0.206 mm, P2 by 0.161 mm, P5 by 0.057 mm, therefore being way contained within the tolerance range. In fact, the deposition process entails position errors for the functional points which are from 4 to 20% of the respective spherical tolerance zones.

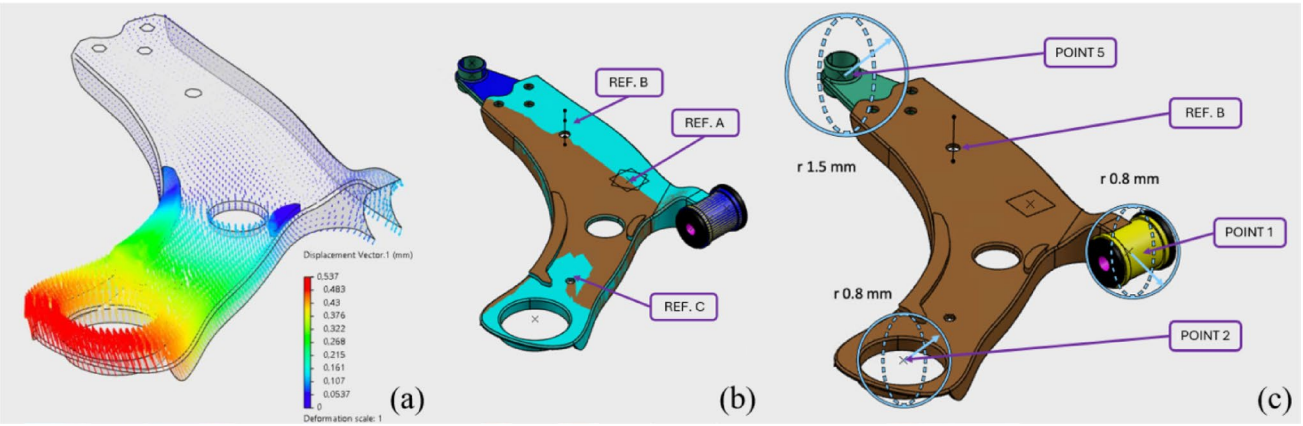

Fig. 13 The nodal displacement vector field to create the deformed geometry (**a**), the alignment procedure of nominal and deformed geometries with datums (**b**), and the verification of the position of the functional points (**c**)

4.1 Potentials, limitations and future work

The DARem framework applied to an actual case study proves to be effective in producing a functional design variant while minimizing the risks of possible failures. The approach is implemented within a commercial CAD platform to exploit seamless integration of product-process design and simulation tasks, therefore enabling practical applications in industrial context.

A critical aspect of the DARem approach is the trade-off between the cost of remanufacturing and that of replacing the manufacturing processes. Certainly, its use is most advantageous for customized products and productions of variants in small batches. The applicability boundaries of DARem can be (i) the material compatibility between the substrate and the depositions (ensuring metallurgical bonding); (ii) the geometrical accessibility for the deposition head and the ability to maintain functionsl tolerances; and (iii) the economic balance between remanufacturing and full replacement, which depends on component size, complexity, and production volume. Furthermore, fatigue and safety considerations become essential, especially in safety-critical applications and under cyclic loading conditions. Fatigue performance of DED parts is strongly influenced by surface finish and post-processing state, but also by build strategies (e.g., build orientation, or deposition rates) [35, 36].

Further works can investigate which are the breakeven points depending on components' complexity and manufacturing process involved. Fatigue-related design checks could be further integrated in DARem, for instance extending Structural Verification outputs to include residual stress and porosity and to adopt strain-life or S–N models for the depositions' materials. Other interesting developments could focus on defining ARem archetypes and process–geometry relationships that establish reference "templates" for practical applications. These aspects could particularly enhance early-stage prototyping and low-volume production, such as advanced pre-series manufacturing in the automotive and aerospace sectors.

5 Conclusions

This research presents a novel and integrated methodology—DARem—that addresses the need for functional upgrades of existing components through DED. The relevance of this concept lies in its alignment with contemporary industrial and sustainability demands, where remanufacturing is increasingly viewed as a strategic solution for enabling design adaptability, reducing time to market, extending product lifecycle, or minimizing resource consumption. The DARem approach couples product and process design based on numerical simulation, its key novelty is the systematic integration of topology optimization, structural and thermo-mechanical simulation, and process planning, all performed within a concurrent engineering framework. This structure allows for early identification and mitigation of potential flaws, reducing the need of physical prototyping and trial-and-error procedures, enabling efficient and reliable manufacturing. In particular, structural FEM and topology optimization are used to define the location and the morphology of material addition where it is structurally most effective. A multi-step thermo-mechanical FEM is used to predict distortions and residual stresses for the associated deposition strategies. By integrating these tasks within a unified CAD/CAE/CAM environment, and leveraging commercial software tools, the seamless transition from design to manufacturing can be practically implemented in industrial applications.

The automotive suspension arm case study exemplifies the methodology's effectiveness. A legacy component was enhanced with 316L steel depositions via DED-LB to improve stress performance while maintaining strict tolerance requirements. FEM results showed a $>50\%$ reduction in peak plastic strain and a $>90\%$ decrease in high-strain areas. The thermo-mechanical simulation guided the selection of the deposition strategy through a Design of Experiments (DoE) approach, yielding distortions well within geometric tolerances, with maximum deviations for functional points limited to 20% of their allowed tolerance zones. The case study confirms the DARem framework's capability to produce functional design variants that meet structural and assembly constraints without altering the original component geometry or manufacturing chain. The approach is particularly well-suited for small-batch, customized, or performance-critical components, offering a compelling alternative to full redesigns or replacements.

Future developments could include: A parametric exploration of DED limits for DARem, to define archetypes for recurring use cases; Economic analyses to define breakeven points for AReM versus traditional manufacturing; Extension to multi-material strategies and functionally graded structures for advanced applications in automotive, aerospace, energy, and tooling sectors.

Appendix A

See Table 2, Table 3.

Table 2 Thermo-mechanical properties of 316L stainless steel

Physical property	Value	Temperature (Kdeg)
Density (kg/m^3)	7990	273.15
	7365	1500
	7127	1645
Elastic modulus (GPa); Poisson's ratio	200; 0.3	273.15
	162; 0.3	800
	510; 0.24	1500
	510; 0.24	1645
Thermal conductivity (W/m·Kdeg)	50	–
Specific heat (kJ/kg·Kdeg)	0.498	273.15
	0.670	1645.15
Latent heat of fusion (kJ/kg)	250	Solidus: 1500 Liquidus: 1645
Thermal expansion coef. (1/Kdeg)	1e-5	273.15

Table 3 Thermo-mechanical properties of a generic steel (substrate)

Physical property	Value	Temperature (Kdeg)
Density (kg/m^3)	7990	273.15
Elastic modulus (GPa); Poisson's ratio	200; 0.3	273.15
Thermal conductivity (W/m·Kdeg)	50	–
Specific heat (kJ/kg·Kdeg)	0.42	273.15
Thermal expansion coef. (1/Kdeg)	7.2e-6	273.15

Appendix B

This chapter analyzes the DOE conducted to study the effects of build strategies in AReM by DED-LB with 316L stainless steel. The goal was to identify process configurations that minimize post-build displacements while controlling build time. The first screening design is a 24 full factorial (FFD) standard experiment (16 runs), allowing estimation of all main effects and two-way interactions. All factors are qualitative (categorical), they are schematized in Fig. 14 and reported together with the associated levels in Table 4. The responses, respectively the maximum displacement extracted by the thermo-mechanical simulation (Y_1 (mm)) and the build time from the behavioral simulation (Y_2 (s)) are reported in Table 5. Simulations were deterministic, uncertainty was handled by comparing results with experiments, and no surrogate models were required since all design points were evaluated. Minimum displacement (primary response) occurred for A=B−A, B=90°, D=LP, while build time reduction occurred through bidirectional (C_2) paths.

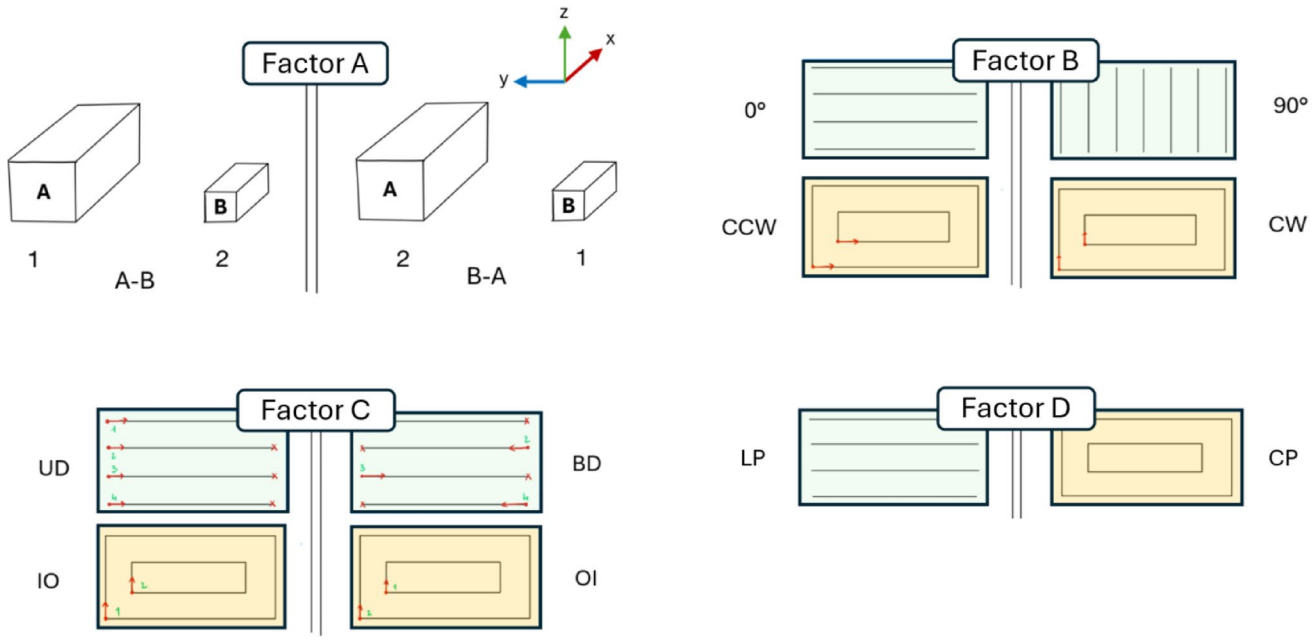

Fig. 14 Overview of the investigated factors and levels in the DED-LB process: the scanning sequence (Factor A) with levels A–B and B–A; the scanning pattern orientation (Factor B) with levels 0° and 90° for line configuration, and clockwise and counterclockwise for concentric patterns; the scanning direction (Factor C) with levels unidirectional/bidirectional or inside-out/outside-in; and the scanning pattern type (Factor D) with line and concentric configurations

Table 4 Factors of first DOE and associated levels

Factor	Symbol	Description	Levels	Notes
Scanning sequence	A	Build order between depositions	L1: A→B; L2: B→A	A larger than B
Scanning pattern orientation	B	Toolpath direction	L1: 0°/CCW (X); L2: 90°/CW (Y)	–
Scanning pattern direction	C	Path progression logic	L1: UD/IO; L2: BD/OI	Depends on pattern type
Scanning pattern type	D	Layer fill strategy	L1: Line (LP); L2: Concentric (CP)	Influences heat distribution

Although deterministic simulation results, the residual variance was estimated from high-order numerical rounding errors, allowing an analytical F-ratio comparison. ANOVA results (Table 6) show that Scanning Pattern Type (D) and Orientation (B) dominate the primary response ($p<0.001$), jointly explaining more than 90% of the total variance (respectively, about 67 and 27%).

To further optimize the process, a second design was performed, fixing D1 (reduced distortion) and C_2 (reduced build time), and introducing two further levels (Fig. 15 and Table 7) to fine-tune the process, thus obtaining a 3^2 FFD. Analysis confirmed A_2 and B_2 as optimal, while simultaneous builds and alternating orientations caused higher variability and distortion.

Key findings include:

- Scanning pattern type (D) dominates distortion: Line patterns reduce warping.
- Orientation (B) strongly influences residual stress: 90° paths (shorter lines) minimize distortion.

Table 6 ANOVA summary for maximum displacement (Y_1)

	SS	df	MS	F	*p*-value
A	0.018	1	0.018	0.9	0.36
B	1.145	1	1.145	57.3	<0.001
C	0.008	1	0.008	0.4	0.53
D	2.814	1	2.814	140.7	<0.001
Residual (Error)	0.220	11	0.020	–	–
Total	4.205	15	–	–	–

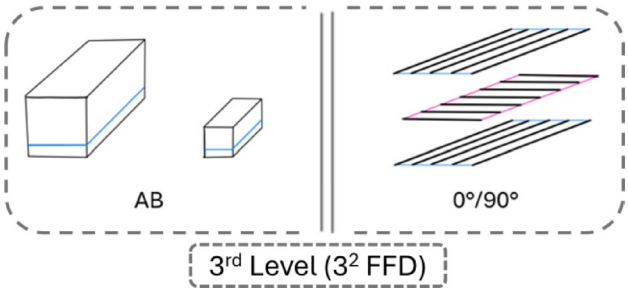

Fig. 15 Additional levels for parallel sequence (AB) and alternating orientation (0°/90°) in the optimization phase

Table 7 Factors of second DOE and associated levels

Factor	Symbol	Description	Levels	Notes
Scanning sequence	A	Build order between depositions	L1: A→B; L2: B→A; L3: AB	AB = parallel
Scanning pattern orientation	B	Toolpath direction	L1: 0° (X); L2: 90° (Y); L3: 0°/90°	0°/90° = alternating

- Bidirectional scanning (C_2) shortens build time with negligible distortion penalties.
- Sequencing (A) affects stress evolution: building the larger deposition last (B−A) is preferable.

Table 5 Responses of the factors—maximum displacement (Y_1 (mm)) and build time (Y_2 (s))

Factor	Y_1 @L1	Y_1 @L2	$\lvert\bar{Y}_1\rvert$	Y_2 @L1	Y_2 @L2	$\lvert\bar{Y}_2\rvert$
A	2.246	2.114	0.133	2913.047	2912.993	0.054
B	2.715	1.645	1.070	2912.144	2913.895	1.751
C	2.224	2.136	0.088	2917.206	2908.834	8.372
D	1.341	3.019	1.678	2790.476	3035.563	245.087

Acknowledgements The authors gratefully acknowledge engg. Carlo Carcioffi, Carlo Laurino, and Tommaso Patuelli for their valuable support, and the "CIM 4.0" Competence Center (Turin, Italy) for resources provision.

Author contributions Conceptualization, E.D.; methodology, E.D and F.P.; validation E.D.; writing—original draft preparation, E.D and F.P.; writing—review and editing, E.D, F.P, and F.L; .; supervision, F.L. All authors read and approved the final manuscript.

Funding Open access funding provided by Università degli Studi di Modena e Reggio Emilia within the CRUI-CARE Agreement. The authors declare that no funds were received during the preparation of this manuscript.

Data availability No datasets were generated or analysed during the current study.

Declarations

Competing interests The authors declare no relevant conflict of interest.

References

1. International Organization for Standardization & ASTM International (2021) ISO/ASTM 52900:2021—Additive manufacturing—General principles—Terminology. ISO. https://www.iso.org/standard/82586.html
2. Ngo TD, Kashani A, Imbalzano G, Nguyen KT, Hui D (2018) Additive manufacturing (3D printing): a review of materials, methods, applications and challenges. Compos B Eng 143:172–196. https://doi.org/10.1016/j.compositesb.2018.02.012
3. Dass A (2019) Moridi, state of the art in directed energy deposition: from additive manufacturing to materials design. Coatings 9(7):418. https://doi.org/10.3390/coatings9070418
4. Jafari D, Vaneker THJ, Gibson I (2021) Wire and arc additive manufacturing: opportuni-ties and challenges to control the quality and accuracy of manufactured parts. Mater Des 202:109471
5. -meter long titanium airplane part is 3D printed in one piece. Accessed 10/09/2020 https://www.openelectronics.org/5-meter-long-titanium-airplane-part-is-3dprinted-in-one-piece/
6. M. Hedges, N. (2006) Calder, Near Net Shape Rapid Manufacture & Repair by LENS®, Cost Effective Manufacture via Net-Shape Processing.In: Meeting Proceedings RTO-MP-AVT. 139. 13–14).
7. Piscopo G, Iuliano L (2022) Current research and industrial application of laser powder directed energy deposition. Int J Adv Manuf Technol 119:6893–6917. https://doi.org/10.1007/s00170-021-08596-w
8. Saboori A, Aversa A, Marchese G, Biamino S, Lombardi M, Fino P (2019) Application of directed energy deposition-based additive manufacturing in repair. Appl Sci 9:3316. https://doi.org/10.3390/app9163316
9. Lalegani Dezaki M, Serjouei A, Zolfagharian A, Fotouhi M, Moradi M, Ariffin MKA, Bodaghi M (2022) A review on additive/subtractive hybrid manufacturing of directed energy deposition (DED) process. Adv Powder Mater. https://doi.org/10.1016/j.apmate.2022.100054
10. Gasser A, Backes G, Kelbassa I, Weisheit A, Wissenbach K (2010) Laser additive manufacturing: laser metal deposition (LMD) and selective laser melting (SLM) in turbo-engine applications. Laser Tech J 7(2):58–63
11. Wilson JM, Piya C, Shin YC, Zhao F, Ramani K (2014) Remanufacturing of turbine blades by laser direct deposition with its energy and environmental impact analysis. J Clean Prod 80:170–178. https://doi.org/10.1016/j.jclepro.2014.05.084
12. BENNETT, Jennifer, DUDAS, Rory, CAO, Jian, EHMANN, Kornel, HYATT, Gregory. Control of Heating and Cooling for Direct Laser Deposition Repair of Cast Iron Components.In: International Symposium on Flexible Automation (ISFA), 2016, 229–236.
13. TORIMS, Toms. (2013) The Application of Laser Cladding to Mechanical Component Repair, Renovation and Regeneration. DAAAM Int Sci Book. 12:587–608
14. Ahn D-G (2011) Applications of laser assisted metal rapid tooling process to manufacture of molding & forming tools—state of the art. Int J Precis Eng Manuf 12(5):925–938
15. Bennett J, Garcia D, Kendrick M, Hartman T, Hyatt G, Ehmann K, You F, Cao J (2019) Repairing automotive dies with directed energy deposition: industrial application and life cycle analysis. J Manuf Sci Eng. https://doi.org/10.1115/1.4042078
16. Leino M, Pekkarinen J, Soukka R (2016) The role of laser additive manufacturing methods of metals in repair, refurbishment and remanufacturing—enabling circular economy. Phys Procedia. https://doi.org/10.1016/j.phpro.2016.08.077
17. Polenz S, Oettel M, López E, Leyens C (2019) Hybrid process chain from die casting and additive manufacturing. Light Des Worldw 12:44–49. https://doi.org/10.1007/s41777-019-0021-8
18. Josten A, Höfemann M (2020) Arc-welding based additive manufacturing for body reinforcement in automotive engineering. Weld World 64:1449–1458. https://doi.org/10.1007/s40194-020-00959-3
19. Wiberg A, Persson J, Ölvander J (2019) Design for additive manufacturing—a review of available design methods and software. Rapid Prototyp J 25(6):1080–1094. https://doi.org/10.1108/RPJ-10-2018-0262
20. Vaneker T, Bernard A, Moroni G, Gibson I, Zhang Y (2020) Design for additive manufacturing: framework and methodology. CIRP Ann 69(2):578–599. https://doi.org/10.1016/j.cirp.2020.05.006
21. Taborda LLL, Maury H, Pacheco J (2021) Design for additive manufacturing: a comprehensive review of the tendencies and limitations of methodologies. Rapid Prototyp J 27:918–966. https://doi.org/10.1108/RPJ-11-2019-0296
22. Egan PF (2023) Design for additive manufacturing: recent innovations and future directions. Designs 7:83. https://doi.org/10.3390/designs7040083
23. Aversa A, Marchese G, Emilio B (2021) Directed energy deposition of AISI 316L stainless steel powder: effect of process parameters. Metals 11:932
24. POGGI, Marina, SALMI, Alessandro, ATZENI, Eleonora, IULIANO, Luca. (2023) Effect of process parameters on AISI

316L single tracks by laser powder directed energy deposition. Procedia CIRP 118:735–740
25. Kahya H, Gurun H, Kucukturk G (2023) Experimental and analytical investigation of the re-melting effect in the manufacturing of 316L by direct energy deposition (DED) method. Metals 13:1144
26. Dalpadulo, E, Pini, F, & Leali, F. "Additive Remanufacturing Integrated Design Approach for Performance Improvement of Automotive Components." Proceedings of the ASME 2022 International Mechanical Engineering Congress and Exposition. Volume 4: Biomedical and Biotechnology; Design, Systems, and Complexity. Columbus, Ohio, USA. October 30–November 3, 2022. V004T06A006. ASME. https://doi.org/10.1115/IMECE2022-97144
27. Liang X, Cheng L, Chen Q, Yang Q, To, (2018) A.C.: a modified method for estimating inherent strains from detailed process simulation for fast residual distortion prediction of single-walled structures fabricated by directed energy deposition. Addit Manuf 23:471–486
28. Dalpadulo E, Pini F, Leali F (2023) Directed Energy Deposition Process Simulation to Sustain Design for Additive Remanufacturing Approaches. In: Gerbino, S., Lanzotti, A., Martorelli, M., Mirálbes Buil, R., Rizzi, C., Roucoules, L. (eds) Advances on Mechanics, Design Engineering and Manufacturing IV. JCM 2022. Lecture Notes in Mechanical Engineering. Springer, Cham. https://doi.org/10.1007/978-3-031-15928-2_93
29. Montgomery D, St C (2017) Design and analysis of experiments, 9th edn. Wiley
30. Cheng M, Zou Xi, Pan Y, Zhou Y, Liu W, Song L (2023) Residual stress control using process optimization in directed energy deposition. Materials 16:6610
31. Ren K, Chew Y, Fuh JYH, Zhang YF, Bi GJ (2019) Thermo-mechanical analyses for optimized path planning in laser aided additive manufacturing processes. Mater Des 162:80–93
32. Elnaz Mirazimzadeh S, Pazireh S, Urbanic J, Hedrick B (2022) Investigation of effects of different moving heat source scanning patterns on thermo-mechanical behavior in direct energy deposition manufacturing. Int J Adv Manuf Technol 120:4737–4753
33. Soffel F, Eisenbarth D, Wegener K (2021) Effect of clad height, substrate thickness and scanning pattern on cantilever distortion in direct metal deposition. Int J Adv Manuf Technol 117:2083–2091
34. Dalpadulo E, Pini F, Gherardini F, Leali F (2025) Directed Energy Deposition Build Strategy Simulation and Optimization for Additive Remanufacturing. In: Manchado del Val, C., Miralbes Buil, R., Peris Fajarnés, G., Moncho Santonja, M., Rizzi, C., Roucoules, L. (eds) Advances on Mechanics, Design Engineering and Manufacturing V. JCM 2024. Lecture Notes in Mechanical Engineering. Springer, Cham. https://doi.org/10.1007/978-3-031-72829-7_55
35. Avanzini A (2023) Fatigue behavior of additively manufactured stainless steel 316L. Materials 16:65. https://doi.org/10.3390/ma16010065
36. Jafor MA, Kinser R, Zhu N, Matalgah K, Allison PG, Jordon JB, Fleck TJ (2025) Influence of deposition rate on fatigue behavior of 316L stainless steel prepared via hybrid laser wire direct energy deposition. Metals 15:543. https://doi.org/10.3390/met15050543